Swift Observations of GRB 080810

K.L. Page (U. Leicester), S.T. Holland (CRESST/USRA/GSFC), D.M. Palmer (LANL), S.D. Barthelmy (GSFC), D.N. Burrows (PSU), P.W.A. Roming (PSU), N. Gehrels (NASA/GSFC) for the Swift Team

1 Introduction

BAT triggered on and located GRB 080810 at 13:10:12UT (trigger=319584; Page et al., GCN Circ. 8080), slewing immediately. A bright afterglow was detected by both the XRT and UVOT, with the best *Swift* position being that determined by the UVOT: RA, Dec (J2000.0) = $23^h\ 47^m\ 10.26^s$, $+00^o\ 19'\ 11.3''$ with an estimated uncertainty of 0.6 arcsec (radius, 90% confidence).

The gamma-ray emission was also seen by GLAST (Meegan et al., GCN Circ. 8100) and INTEGRAL/SPI-ACS (V. Beckmann, priv. comm.); all SPI-ACS events can be viewed at http://isdc.unige.ch/Soft/ibas/ibas_acs_web.cgi.

The optical afterglow was detected by a large number of observatories (KANATA – Ikejiri et al., GCN Circ. 8081, Uemura et al., GCN Circ. 8085; ROTSE-III – Rykoff, GCN Circ. 8084; RTT150 – Burenin et al., GCN Circ. 8088, Galeev et al., GCN Circ. 8098; 1.5 m OSN – de Ugarte Postigo et al., GCN Circ. 8090; Kanazawa – Okuma et al., GCN Circ. 8091; Danish 1.5 m on La Silla – Thoene et al., GCN Circ. 8106; D50 telescope in the Czech Republic – Kocka et al., GCN Circ. 8092; Liverpool and Faulkes North Telescopes – Guidorzi et al., GCM Circ. 8093, 8099; Mt.Terskol Observatory – Andreev et al., GCN Circ. 8094; MITSuME – Yoshida et al., GCN Circ. 8097; CrAO – Rumyantsev et al., 8105), while the redshift was measured to be 3.35 by Prochaska et al. (GCN Circ. 8083) and confirmed by RTT150 (Burenin et al., GCN Circ. 8088) and NOT (de Ugarte Postigo et al., GCN Circ. 8089).

Swift observations continued until 17th August 2008, when the target became Moon constrained.

2 BAT Observation and Analysis

The BAT ground-calculated position is RA, Dec = 356.783, 0.310 degrees, which is equivalent to

RA(J2000) = $23^h\ 47^m\ 08.0^s$
Dec(J2000) = $+00^o\ 18'\ 35.1$"

with an uncertainty of 1.2 arcmin, (radius, sys+stat, 90% containment). The partial coding was 68%.

The mask-weighted light curve (Figure 1) shows a cluster of overlapping peaks starting at $\sim$ T$-$20 s, the tallest being at $\sim$ T+25 s, and the last ending at $\sim$ T+120 s. T_{90} (15-350 keV) is 106 $\pm$ 5 s (estimated error including systematics).

The time-averaged spectrum from T$-$21.2 to T+111.4 s is best fitted by a simple power-law model. The power law index of the time-averaged spectrum is 1.34 $\pm$ 0.06. The fluence in the 15–150 keV band is $(4.6 \pm 0.2) \times 10^{-6}$ erg cm^{-2}. The 1-s peak photon flux measured from T+24.68 s in the 15–150 keV band is 2.0 $\pm$ 0.2 ph cm^{-2} s^{-1}. All the quoted errors are at the 90% confidence level.

The results of the batgrbproduct analysis are available at http://gcn.gsfc.nasa.gov/notices_s/319584/BA/

3 XRT Observations and Analysis

The XRT began observing the burst 76 s after the trigger. Using 1614 s of XRT Photon Counting (PC) mode data and 3 UVOT images, an astrometrically corrected X-ray position (using the XRT-UVOT alignment and matching UVOT field sources to the USNO-B1 catalogue) was derived: RA, Dec = 356.79418, +0.32000 degrees, which is equivalent to:

RA (J2000) = $23^h\ 47^m\ 10.60^s$
Dec (J2000) = $+00^o\ 19'\ 12.0"$

with an uncertainty of 1.4 arcsec (radius, 90% confidence).

The WT data show a number of flares, with the strongest peaking around 107 and 209 s after the trigger; the first of these is also visible in the BAT data. The PC data in later orbits can be modelled with a broken power-law, with $\alpha \sim 0$ until 5.9 ± 0.4 ks after the trigger, at which point the slope steepens to $\alpha = 1.76^{+0.10}_{-0.08}$. There is also a late-time rebrightening seen, around 100 ks.

There is strong spectral evolution throughout the first orbit, as is typical for flaring activity. A spectrum extracted from the PC mode data in the second orbit (the plateau phase) can be modelled with a power-law of $\Gamma = 1.95 \pm 0.07$ absorbed by the Galactic column of $N_H = 3.28 \times 10^{20}$ cm^{-2}. After the temporal break, the photon index becomes $\Gamma = 2.00 \pm 0.09$, so there is no sign of spectral evolution after the early flares cease.

The counts to observed flux conversion is 1 count s^{-1} = 3.8×10^{-11} erg cm^{-2} s^{-1}.

Detailed light-curves in both count rate and flux units are available in both graphical and ASCII formats from http://www.swift.ac.uk/xrt_curves/00319584/.

4 UVOT Observation and Analysis

The UVOT observed the burst starting from 65 s after the BAT trigger, with settled observations starting at T+85 s. The optical afterglow was detected in the v, b and white filters.

The refined UVOT source position is

RA (J2000.0) = $23^h\ 47^m\ 10.26^s$
Dec (J2000.0) = $+00^o\ 19'\ 11.3''$

with an estimated uncertainty of 0.6 arcsec (radius, 90% confidence).

Fig. 3 plots the UVOT light-curve in all filters. The non-detection in u, coupled with a detection in b, suggests a redshift of between approximately 2.7 and 3.7, consistent with the measured value of z = 3.35 (Prochaska et al., GCN Circ. 8083; Burenin et al., GCN Circ. 8088; de Ugarte Postigo et al., GCN Circ. 8089). There is a marginally-detected bump in the white data, close in time to the rebrightening seen in the XRT (Fig. 2).

Filter	Tstart	Tstop	Exposure	Mag
white	85	185	98	14.63 ± 0.07
v	191	459	264	14.06 ± 0.06
b	4432	4632	197	17.85 ± 0.08
u	4227	68 686	727	>21.4
uvw1	4022	68 283	3099	>22.3
uvm2	3817	62 540	3229	>22.2
uvw2	4843	50 866	1510	>22.0

Table 1: UVOT magnitudes in all filters. 3σ upper limits are given where the afterglow was not detected.

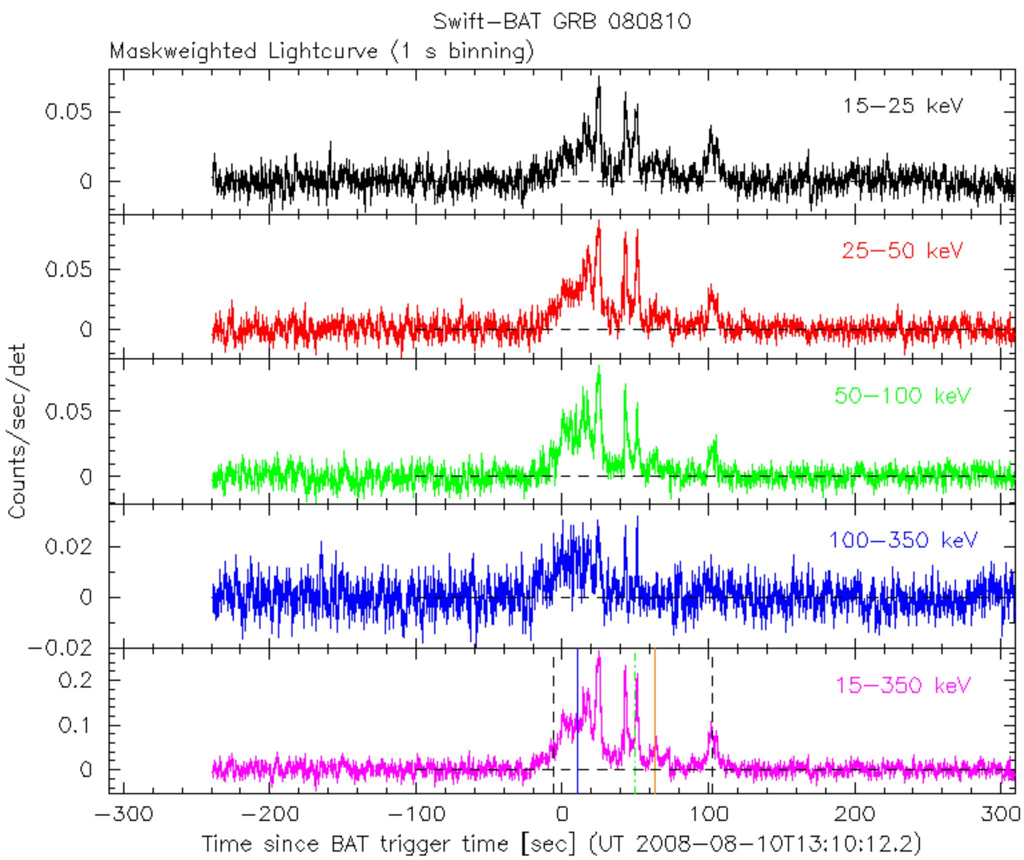

Figure 1: BAT light-curve. The mask-weighted light-curve in the 4 individual plus total energy bands. The units are counts/s/illuminated-detector (note illum-det = 0.16 cm^2).

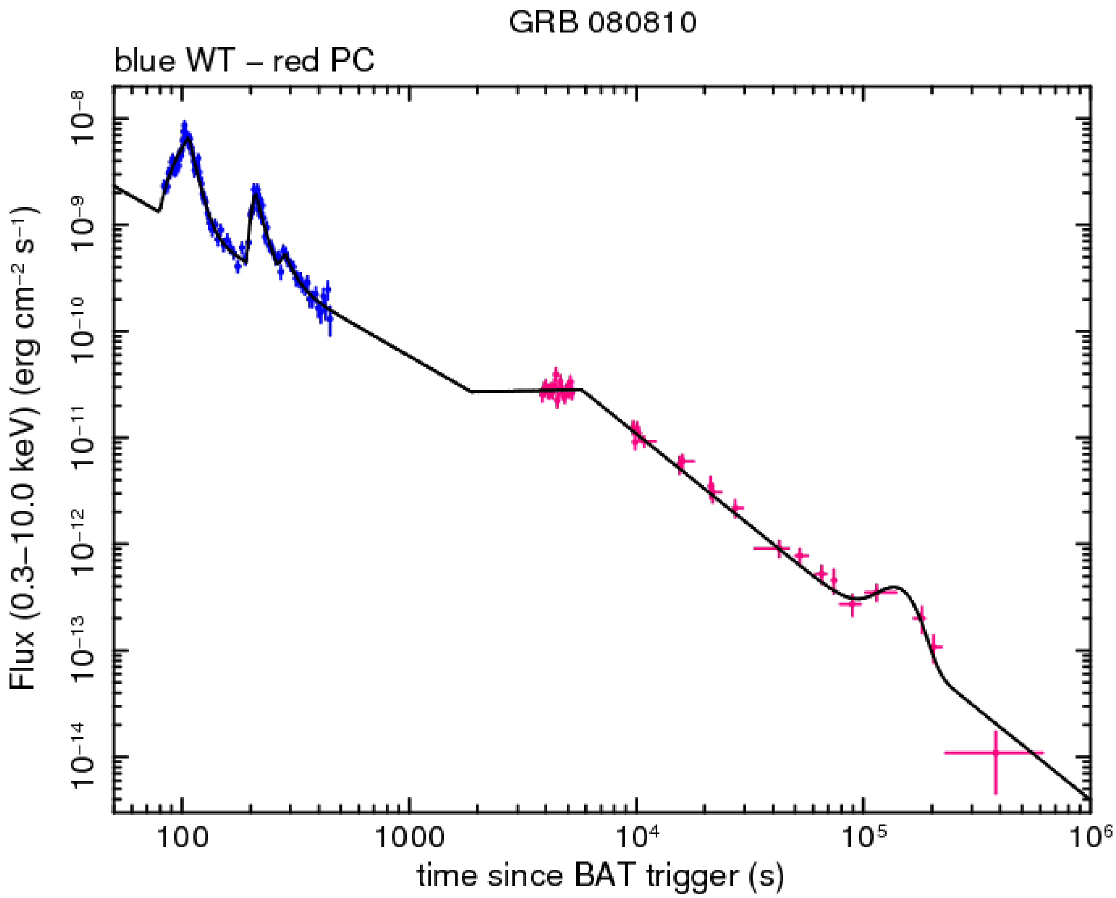

Figure 2: XRT flux light-curve. Windowed Timing mode is shown in blue, Photon Counting mode in red. The approximate counts to flux conversion is 1 count s^{-1} = 3.8×10^{-11} erg cm^{-2} s^{-1}.

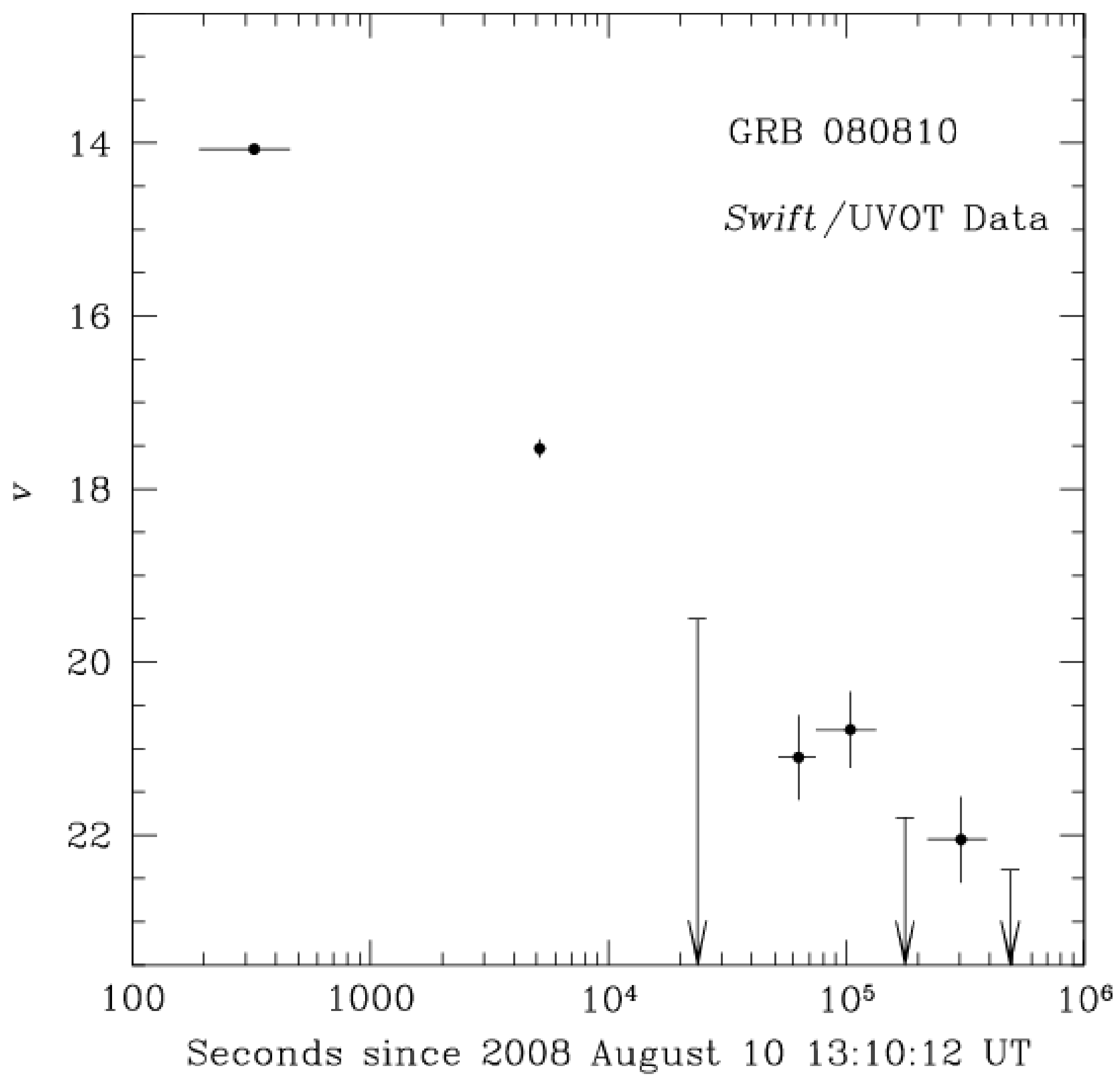

Figure 3: UVOT light-curve. Magnitudes (and 2-sigma upper limits) for the v-band data.